

SUPPORTING INFORMATION: Photoluminescence imaging of whole zircon grains on a petrographic microscope— an underused aide for geochronologic studies

Ryan J. McAleer ^{1,*}, Aaron M. Jubb ², Paul C. Hackley ², Gregory J. Walsh ³, Arthur J. Merschat ¹, Sean P. Regan ^{4,5}, William C. Burton ¹ and Jorge A. Vazquez⁶.

¹ U.S. Geological Survey, Florence Bascom Geoscience Center, 12201 Sunrise Valley Dr., Reston, VA 20192, USA; amerschat@usgs.gov (A.J.M.); bburton@usgs.gov (W.C.B.)

² U.S. Geological Survey, Eastern Energy Resources Science Center, 12201 Sunrise Valley Dr., Reston, VA 20192, USA; ajubb@usgs.gov (A.M.J.); phackley@usgs.gov (P.C.H.)

³ U.S. Geological Survey, Florence Bascom Geoscience Center, 87 State Street Room 228, PO Box 628, Montpelier, VT 05602, USA; gwalsh@usgs.gov

⁴ Department of Geosciences, University of Alaska Fairbanks, Fairbanks, Alaska 99775, USA; sregan5@alaska.edu

⁵ Geophysical Institute, University of Alaska Fairbanks, Fairbanks, Alaska 99775, USA; sregan5@alaska.edu

⁶ U.S. Geological Survey, 345 Middlefield Road, Mail Stop 910, Menlo Park, CA 94025, USA; jvazquez@usgs.gov

* Correspondence: rmcaleer@usgs.gov

This supplementary information includes additional examples of correlative microscopy from zircon grains in samples PB515, GP1104 and HD-18-1 (Figures S1-S5). Trace element data from spot locations annotated in these figures is also given in Table S1. We also provide the data used to plot Figure 8 in the in Table S2.

Our measured FWHM values for Dy³⁺ sublevel I, Dy³⁺ sublevel II, and the $\nu_3(\text{SiO}_4)$ stretching mode are plotted along with the data of Lenz and Nasdala [1] in Figure S6. Our data show the same positive correlations between FWHM and α -dose for all three parameters— although the scatter is greater. Additionally, the slope of the sublevel I correlation is steeper than the slope of the sublevel II correlation as noted by Lenz and Nasdala [1].

Tables

Table S2. Data plotted in Figure 8 of the main text. Y = yellow PL, R = red PL, Y/C = zoned from yellow PL to colorless.

Sample	Figure	PL Color	U (ppm)	Th (ppm)	U/Pb Age ^a (Ma)	ZFT Age ^b (Ma)	U/Pb α -dose ^c (α /g)	ZFT α -dose ^d (α /g)
PB515	2d	Y	180	120	430	186	3.02E+17	1.28E+17
PB515	2e	R	1300	470	435	186	2.07E+18	8.66E+17
PB515	2e	Y	27	0	381	186	3.46E+16	1.66E+16
PB515	2f	Y	17	0.4	390	186	2.24E+16	1.05E+16
PB515	2g	R	690	130	442	186	1.08E+18	4.42E+17
PB515	S3a	Y	65	0	363	186	7.92E+16	3.99E+16
PB515	S3a	R	690	240	431	186	1.09E+18	4.58E+17
PB515	S3a	Y	107	0	377	186	1.36E+17	6.57E+16
PB515	S3b	Y	35	0	371	186	4.36E+16	2.15E+16
PB515	S3b	R	575	239	415	186	8.83E+17	3.87E+17
PB515	S3b	R	823	431	441	186	1.38E+18	5.67E+17
PB515	S3c	Y	100	1	371	186	1.25E+17	6.15E+16
PB515	S3c	R	2127	494	436	186	3.30E+18	1.38E+18
GP1104	5d	R	720	180	1167	513	3.24E+18	1.33E+18
GP1104	5e	R	390	120	1116	513	1.69E+18	7.30E+17
GP1104	5e	Y	130	48	1132	513	5.79E+17	2.47E+17
GP1104	5f	R	920	7.9	1083	513	3.61E+18	1.61E+18
GP1104	5f	Y	52	27	1129	513	2.38E+17	1.02E+17
GP1104	5f	R	390	8	1034	513	1.46E+18	6.85E+17
GP1104	5g	Y	69	25	1222	513	3.34E+17	1.31E+17
GP1104	5g	R	590	4.6	1116	513	2.40E+18	1.03E+18
GP1104	S4d	R	700	8	1039	513	2.63E+18	1.23E+18
GP1104	S4d	R	1000	50	1005	513	3.65E+18	1.77E+18
GP1104	S4e	Y	100	30	1173	513	4.57E+17	1.87E+17
GP1104	S4e	R	300	5	1052	513	1.14E+18	5.27E+17
HD-18-1	S5a	Y/C	163	96	741	286	4.77E+17	1.77E+17
HD-18-1	S5c	Y/C	135	61	747	286	3.88E+17	1.42E+17
HD-18-1	S5d	Y/C	186	106	734	286	5.37E+17	2.01E+17

^a U/Pb ages are the ²⁰⁶Pb/²³⁸U age for PB515 and HD-18-1 and the ²⁰⁶Pb/²⁰⁷Pb age for GP1104. Ages are in Ma.

^b Zircon Fission Track (ZFT) ages are from the literature [2-4].

^c α -dose assuming complete retention of PL inducing defects following crystallization [5].

^d α -dose assuming complete retention of PL inducing defects following cooling through the closure temperature for the annealing of fission tracks in zircon.

Figures

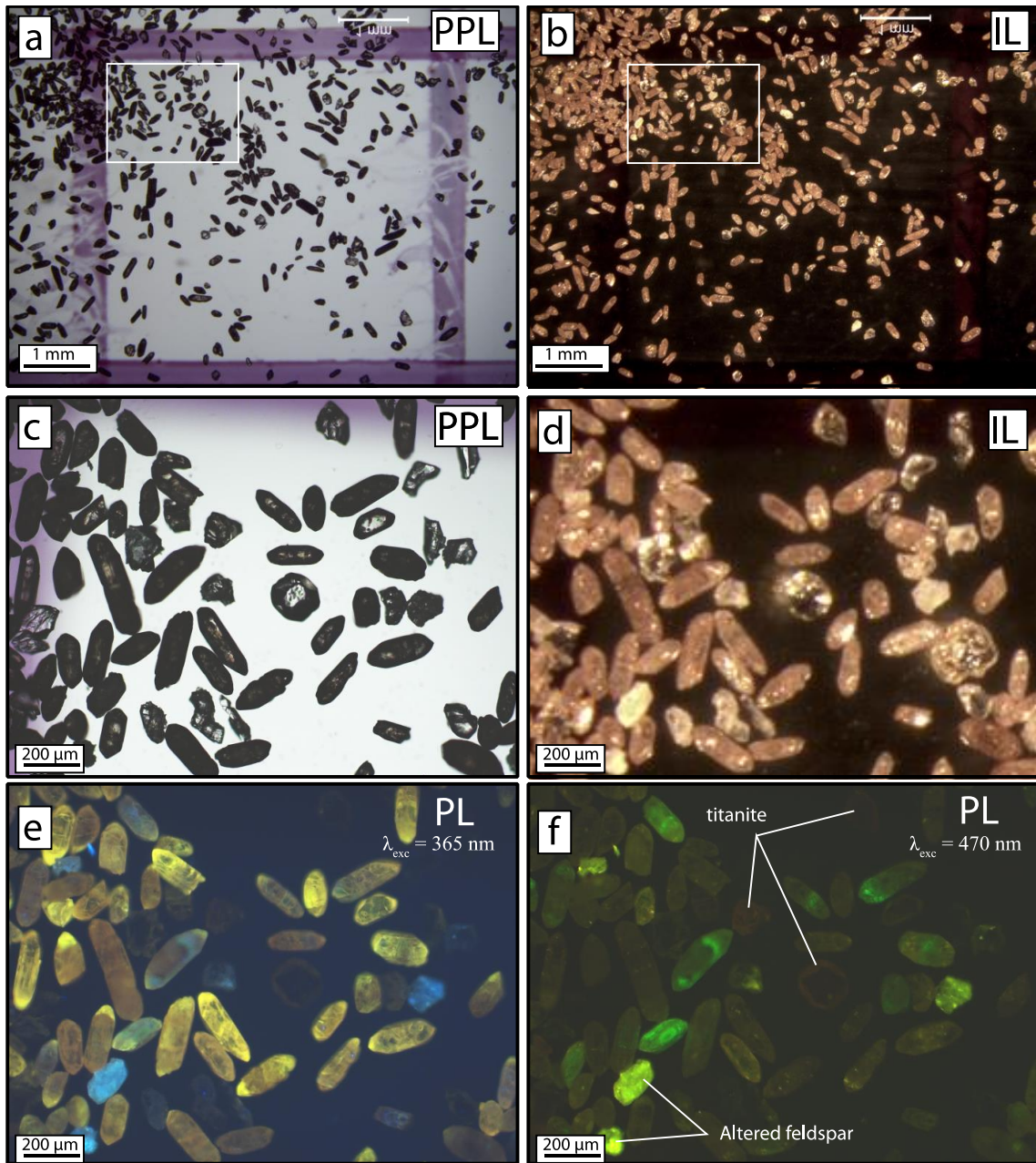


Figure S1. Correlative microscopy of heavy mineral separates from sample PB515. (a)-(b) Correlative PPL and IL images at low magnification. (c)-(f) ~50x correlative images under PPL, IL, 365 nm, and 470 nm excitation, respectively. Grains were dispersed on a glass slide with a square ~5 x 5 mm grid drawn on the back side of the slide. Images A, B, and D were taken on a Leica Z16 stereoscope. The slide was then transferred to a Zeiss AxioImager petrographic scope and the images in (c), (e), and (f) were taken. Grains may have shifted slightly between the two image sets.

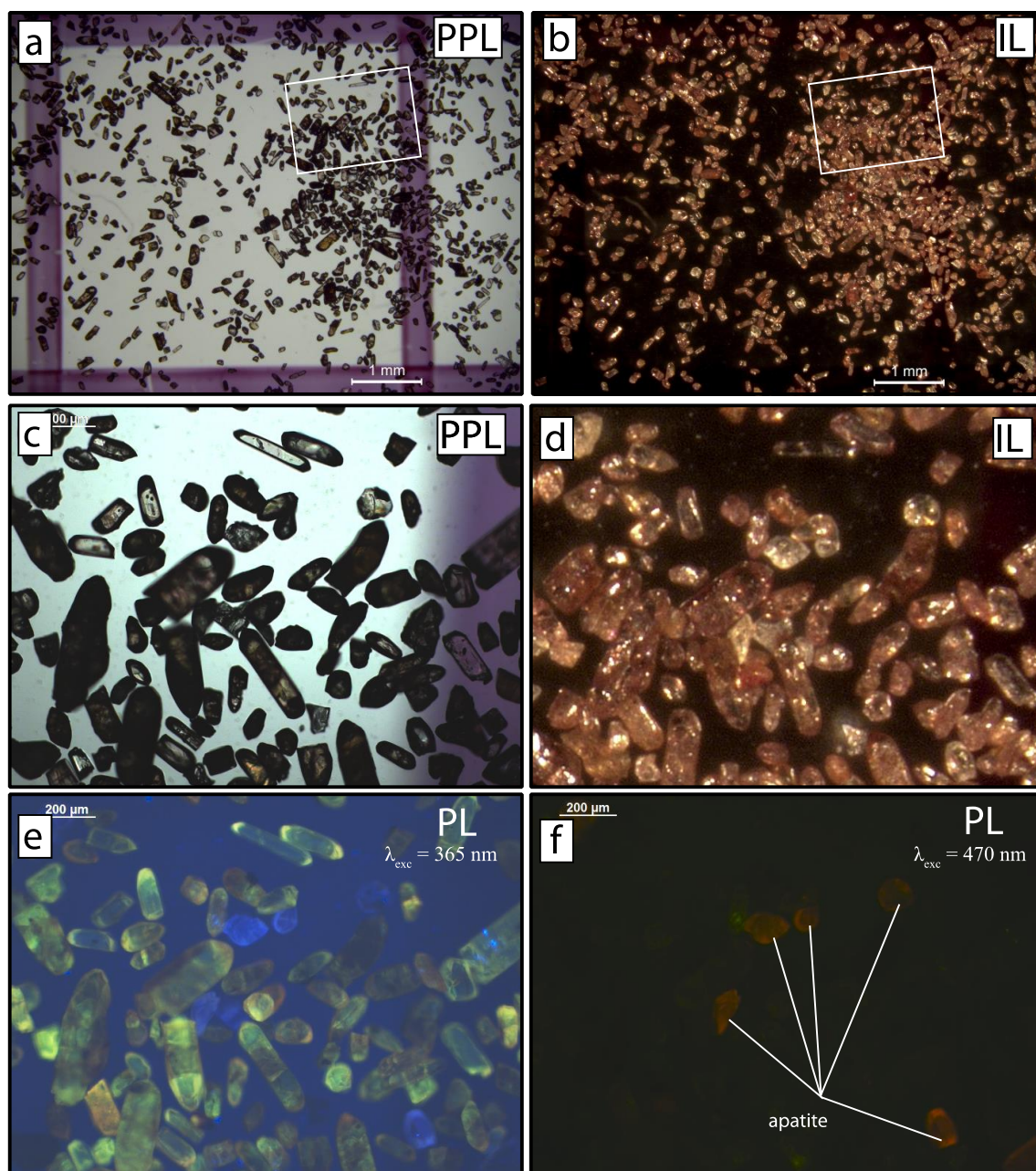


Figure S2. Correlative microscopy of heavy mineral separates from sample GP1104. (a)-(b) correlative PPL and IL images at low magnification. (c)-(f) ~50x correlative images under PPL, IL, 365 nm, and 470 nm excitation, respectively. Grains were dispersed on a glass slide with a square ~5 x 5 mm grid drawn on the back side of the slide. Images (a), (b), and (d) were taken on a Leica Z16 stereoscope. The slide was then transferred to a Zeiss Axiomager petrographic scope and the images in (c), (e), and (f) were taken. Grains may have shifted slightly between the two image sets.

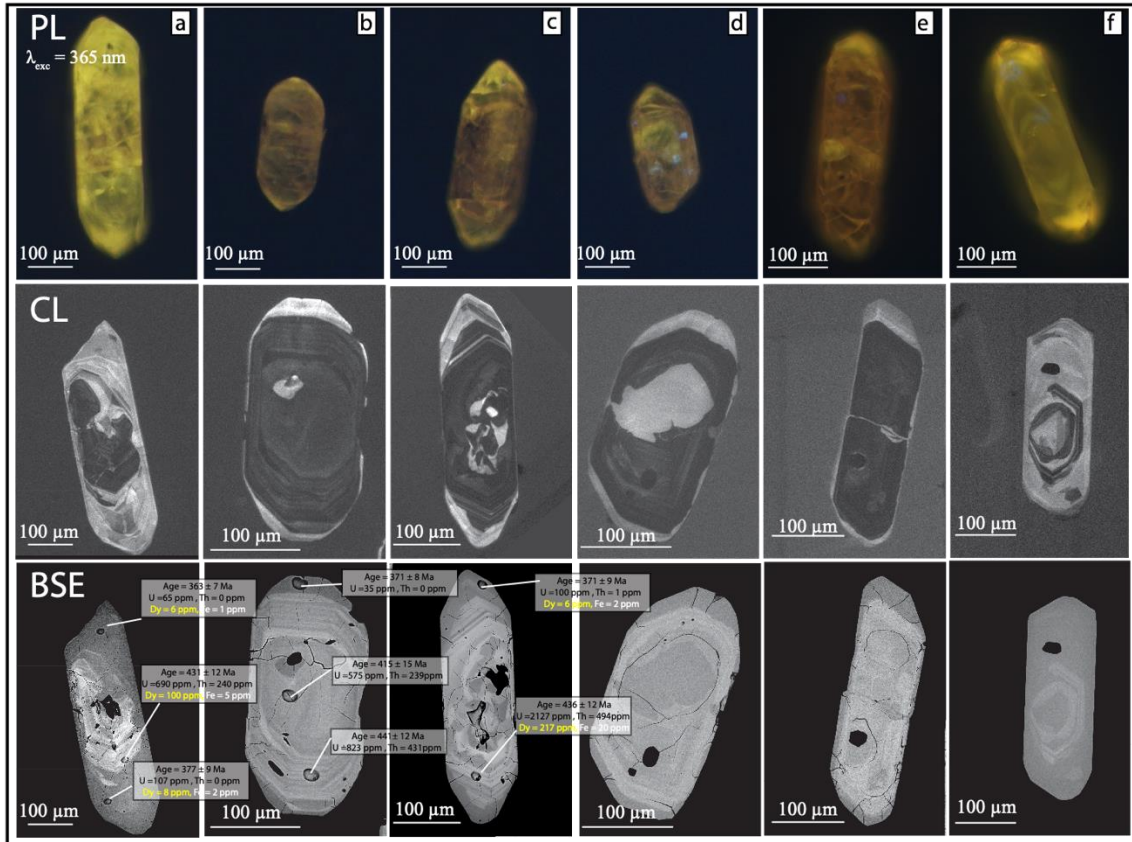


Figure S3. Additional correlative whole grain PL and CL+BSE images from cross sections of the same zircon grains from sample PB515. Grains (a)-(c) were also analyzed by SHRIMP methods, grains (d)-(f) were mounted but not analyzed. Grain (a) is largely replaced by yellow PL low U+Th zircon, grains (b)-(e) also show evidence of replacement as indicated by less pervasive zones of yellow PL zircon in and around zones of red PL. The yellow PL geometry includes overgrowths, small and large embayments, and veins. Grain (f) exhibits oscillatory zoning between yellow and limited to no PL. Faint red PL is visible in the core of grains (a) and (f).

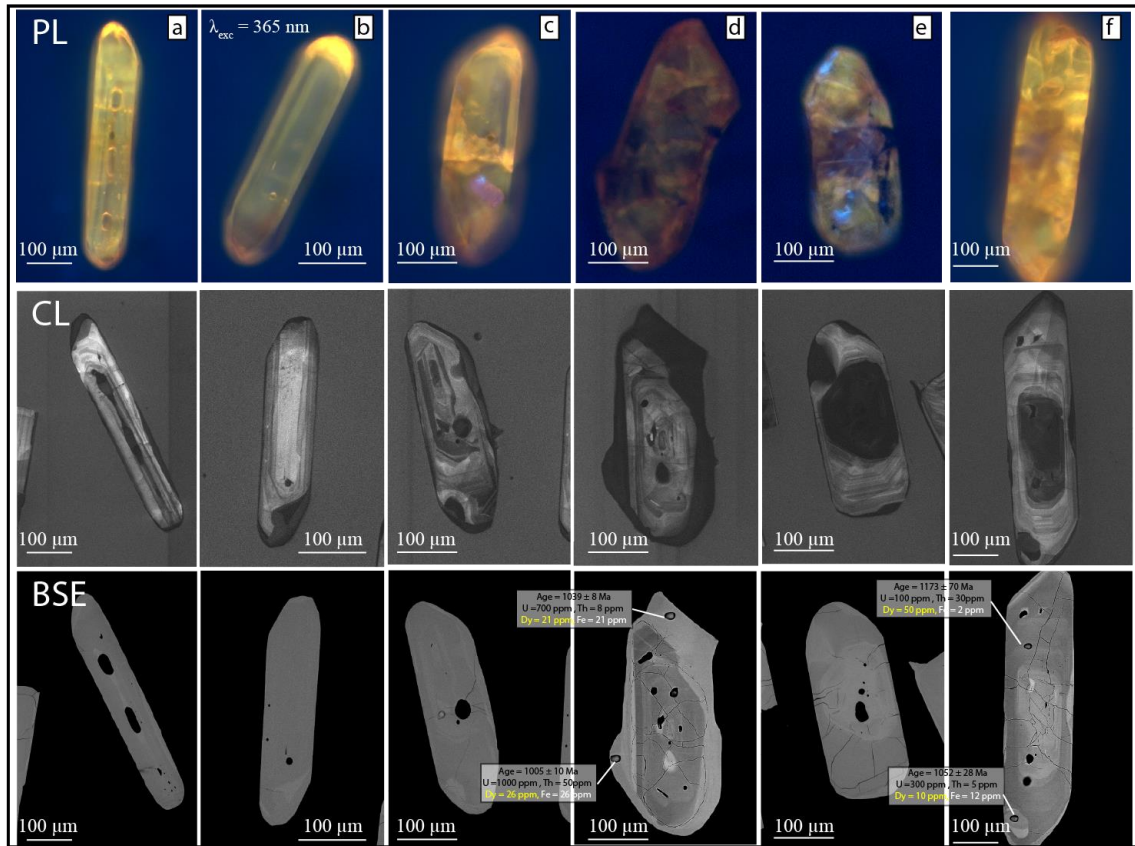


Figure S4. Additional correlative whole grain PL and CL+BSE images from images from cross sections of the same zircon grains from sample GP1104. Grains (d) and (f) were also analyzed by SHRIMP methods. Grains (a) and (b) are of high optical clarity and faint zoning in the yellow PL is present. Both grains also have narrow red PL rims. Grain (c) has a blue PL inclusion that is probably apatite. Grain (d) is weakly luminescent and has dark red rims and that are correspondingly dark in CL. Grains (e) and (f) each have blue/red inner cores that are dark in CL, and yellow PL mantles that are bright in CL and exhibit oscillatory zoning.

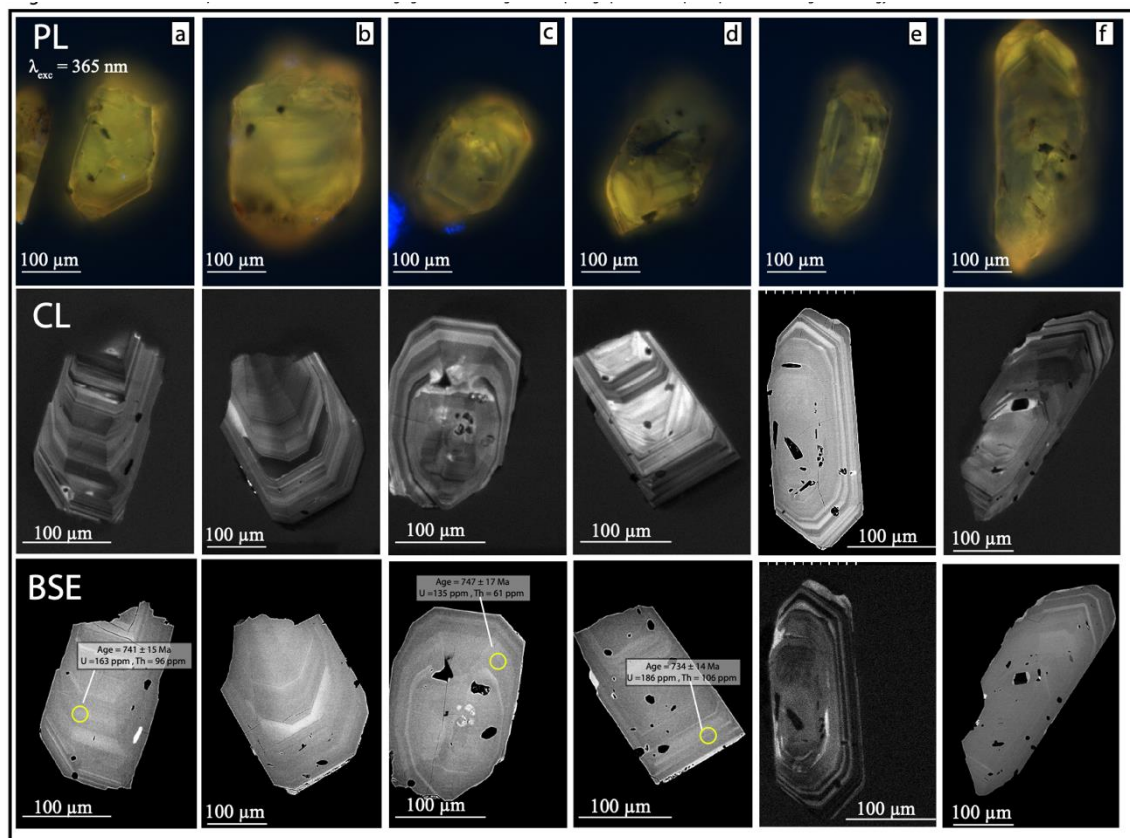


Figure S5. Additional correlative whole grain PL and CL+BSE images from images from cross sections of the same zircon grains from sample HD-1-18. All grains show some degree of oscillatory zoning between bright and faint yellow PL. Bright yellow zones are bright in CL and dark in BSE. External grain shapes do not match exactly because some grains were not polished to exactly 1/2 thickness. Most grains from this sample were optically clear and un-fractured. These conditions result in visibility of finer scale zoning in PL response.

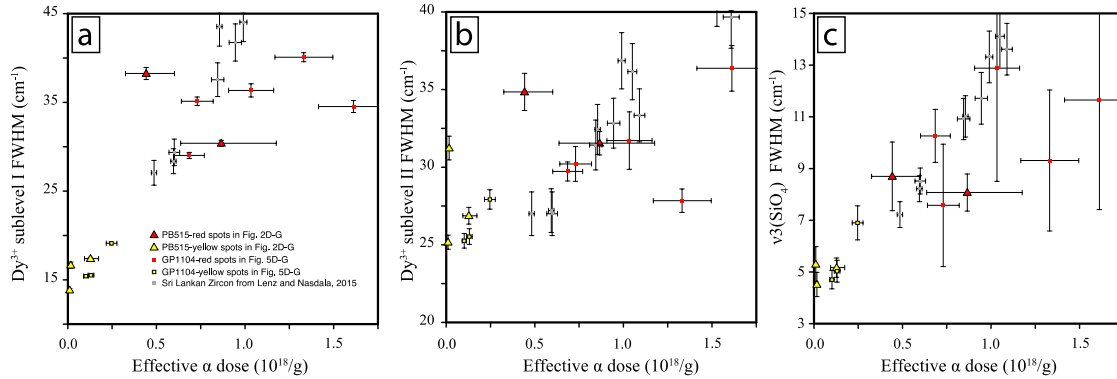


Figure S6. (a) Full width at half max (FWHM) of the Dy³⁺ sublevel I peak vs cumulative alpha dose for the data presented in Table 1 and Figures 2 and 5. (b) FWHM of the Dy³⁺ sublevel II peak vs cumulative alpha dose. (c) FWHM of the $\nu_3(\text{SiO}_4)$ Raman stretching band vs cumulative alpha dose. Data from this study are plotted using regional zircon fission track ages to calculate alpha doses (PB515: 186 +65.6/-48.6 Ma; GP1104: 513 ± 60 Ma) [2-4]). Data marked with grey squares are from Lenz and Nasdala[1] and effective doses were calculated using the U/Pb dose and a correction factor of 0.55 [1,5].

References

1. Lenz, C., and Nasdala, L. (2015) A photoluminescence study of REE³⁺ emissions in radiation-damaged zircon. *American Mineralogist*, 100, 1123–1133.
2. Montario, M.J., Marsellos, A.E., and Garver, J.I. (2008) Annealing of radiation damage in a Grenville zircon from the eastern Adirondacks, NY state. In *Proceedings of the 11th International Conference on Thermochronometry (Anchorage, AK, 2008)* pp. 174–176.
3. Naeser, C.W., Naeser, N.D., Newell, W.L., Southworth, S., Edwards, L.E., and Weems, R.E. (2016) Erosional and depositional history of the Atlantic passive margin as recorded in detrital zircon fission-track ages and lithic detritus in Atlantic Coastal plain sediments. *American Journal of Science*, 316, 110–168.
4. Roden-Tice, M.K., and Wintsch, R.P. (2002) Early Cretaceous Normal Faulting in Southern New England: Evidence from Apatite and Zircon Fission-Track Ages. *The Journal of Geology*, 110, 159–178.
5. Nasdala, L., Reiners, P.W., Garver, J.I., Kennedy, A.K., Stern, R.A., Balan, E., and Wirth, R. (2004) Incomplete retention of radiation damage in zircon from Sri Lanka. *American Mineralogist*, 89, 219–231.